In situ electrochemical characterization of lithium-alloying materials for rechargeable anodes in lithium batteries

S. Machill, D. Rahner *

Dresden University of Technology, Institute of Physical Chemistry and Electrochemistry, Mommsenstrasse 13, 01062 Dresden, Germany

Abstract

In situ electrochemical techniques can be used to investigate the intercalation process of lithium into several inserting materials used in rechargeable lithium battery anodes. Alloying materials on the basis of aluminium, with the addition of small portions of a second metal such as nickel or manganese, are especially examined. The chemical diffusion coefficient of lithium was estimated using the potentiostatic transient technique. Chronoamperometry gives information on the diffusion process related to the chemical composition, grain structure and crystallinity of the alloying material. The measurements have been carried out in a 1 M $LiClO_4$/propylene carbonate solution at room temperature.

Keywords: Lithium alloys; Rechargeable lithium batteries; Anodes

1. Introduction

The use of lithium in rechargeable batteries is a matter of rising interest due to the high energy content of lithium, its small ionic radius and its high mobility in cathode materials. A worldwide interest can be observed in the development of rechargeable lithium batteries. But the use of lithium in secondary batteries is not without problems. High energy densities could only be observed in secondary batteries with pure lithium as anode material. During charging lithium is often deposited in a dendritic form.

The cycleability of the lithium electrode can be improved by the use of lithium-inserting materials. The most common alloys are lithium–carbon and lithium–aluminium. Other suitable alloying materials or substrates are Sn, Pb, Au, Pt, Zn, Cd, Mg, Hg, Bi, Sb, As and others.

The anodes based on Li–Al alloys can be cycled up to 1000 times depending on the cycling conditions. One should emphasize that the depth-of-discharge reaches only 1 to 10% of the value of the comparable primary lithium battery.

Using substrate-forming alloys or intercalation compounds with lithium the reactivity against the electrolyte or the solvent can be decreased. Therefore, the lithium

in the host material will be 'shielded' and formation of dendrites will be reduced or avoided if the diffusion velocity inside the host material is high enough. However, a potential shift occurs and leads to a decrease in the energy and power density. For some purposes the increase in cycleability compensates these disadvantages.

The diffusion of lithium in the alloy matrix determines the charge/discharge rate of the battery and limits its use as a low- or high-rate cell. The diffusion process itself is determined by the nature of the host material and its morphology.

The main problems of lithium-alloy electrodes are connected with the significant differences in volume between the pure basis material and the formed lithium alloy. Therefore, during cycling mechanical stress and cracks are induced to these volume differences (AlLi 96.8% [1] in relation to the host lattice). In the case of carbon, the volume differences during the formation of LiC_6 is only 9.4% [2]. Carbon is therefore the most favoured host material in the last years.

Another way for improving the cycleability of Li–Al alloys is the method of pre-alloying the aluminium host by other metals which are soluble in aluminium or form intermetallic compounds with it, but do not form alloys with lithium, such as nickel. In this way, one expects to create an alloy matrix of modified grain size

---

* Corresponding author.

with stabilizing properties towards 'mechanical stressing' during charge/discharge processes of lithium.

2. Experimental

The preparation of the test cells was carried out as described in our previous papers [3,4]. All kinds of metals used have been of 99.99% purity. The contents of the second metal in the binary aluminium alloys varied between pure aluminium and 42 mass% of nickel and 25.3 mass% of manganese. The various metal electrodes have been prepared from small cylinders with a diameter of 5 mm (surface area: 0.196 cm²) and have been embedded in a Teflon holder. The metal surface was mechanically polished. Both the counter and the reference electrodes were lithium pellets pressed onto nickel nets. The electrolyte solution was prepared from propylene carbonate (Merck) distilled and stored over molecular sieves 4A, and LiClO$_4$ (Merck) gradually dried under vacuum. The content of water could therefore be decreased to 20–30 ppm.

EG&G Model 273A potentiostat in connection with a computer system was used for the electrochemical measurements.

3. Results and discussion

The rate-determining step of the insertion of lithium in lithium-alloying materials is the diffusion in the host lattice. It can be studied by potentiostatic transient methods. This intercalation process can be divided into three parts, depending on the limiting step [5]:

(i) electrochemical incorporation;

(ii) diffusion of the incorporated element in the growing layer of the intermetallic compound, and

(iii) chemical affinity between the metals.

The diffusion process inside the solid state can be described by the Cotrell equation:

$$i = zF(c_{Li}^* - c_{Li}) \sqrt{\frac{D}{\pi t}} \qquad (1)$$

In this case, the measured current density i should monotonously be decreased by $1/\sqrt{t}$ (Fig. 1). Potentiostatic measurements on aluminium and its nickel and manganese alloys give sometimes unusual answer functions. These current–time transients can be interpreted as follows.

In the first step, the discharged lithium ions on top of the metal surface are soluted in the aluminium matrix until the limiting concentration of 2.6 at.% for forming the α-LiAl phase has been reached. It is well known that lithium inside the α-LiAl phase moves very slowly $(D \approx 10^{-11}$ cm²/s). During this starting period even
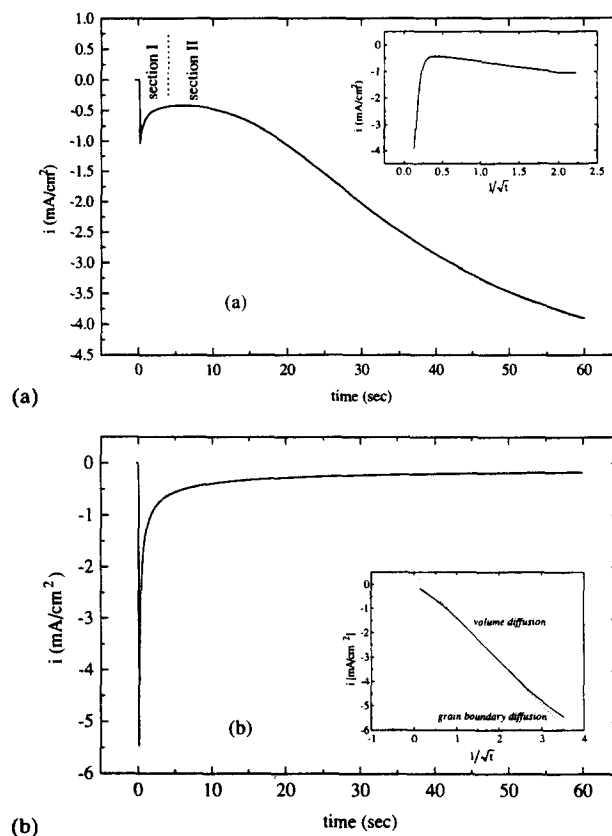

Fig. 1. (a) Potentiostatic transient and Cotrell linearization for aluminium free lithium (potential shift from rest potential to $E=0$ mV vs. Li; 1 M LiClO$_4$/PC). (b) Potentiostatic transient and Cotrell linearization for aluminium charged with 3.6 C/cm² lithium (potential shift from rest potential to $E=0$ mV vs. Li; 1 M LiClO$_4$/PC).

lithium can be plated on the electrode surface if the diffusion rate inside the host material is lower than the deposition rate. With increasing lithium content a new phase (β-LiAl with 50 at.% Li) is growing around the α-LiAl nuclei. The rate of diffusion velocity inside the β-LiAl phase is higher than in the α-LiAl phase and causes a higher current density for the incorporation of lithium. Now, the lithium concentration is increasing from 2.6 to 50 at.%. The nuclei are growing three-dimensionally [6] and the incorporation kinetics follows a cubic law $[i \sim f(t^3)]$.

It should be emphasized that the influence of the microstructure on the observed kinetics has to be considered. The diffusion process inside a polycrystalline material strongly depends on the microstructure and grain-size distribution [7]. One has to distinguish the diffusion in the bulk (volume diffusion) of a grain and the diffusion at the grain boundaries. At the lithiated substrates we can recognize these two kinds of diffusion by different slopes in the linearized form of the Cotrell equation. The diffusion velocity at the grain boundaries exceeds the volume diffusion by some orders of magnitude due to the lowered activation energy at the strongly disordered phase boundaries.

Additional alloying with elements which preferably segregate at grain boundaries (e.g. nickel) should increase the diffusion rate of lithium. Therefore, an accurate knowledge of the concentration of grain boundaries and their distribution as well as of the lithium concentration on the electrode surface is necessary for an exact determination of the diffusion coefficients.

3.1. Chronoamperometry on lithium alloying substrates on the basis of aluminium

Potentiostatic current transients have been measured on Al, AlMn and AlNi substrates under two conditions: free of lithium and pre-charged with lithium. Fig. 1 shows the current–time response of pure aluminium (Fig. 1(a) before any lithium incorporation, Fig. 1(b) after lithium incorporation with 1 mAh/cm²) and the Cotrell linearization. In the case of AlMn and AlNi substrates the same interrelation has been given in Fig. 2.

It will be shown that the diffusion coefficients for aluminium can be approximately estimated. According to Eq. (1) the slope m is given by:
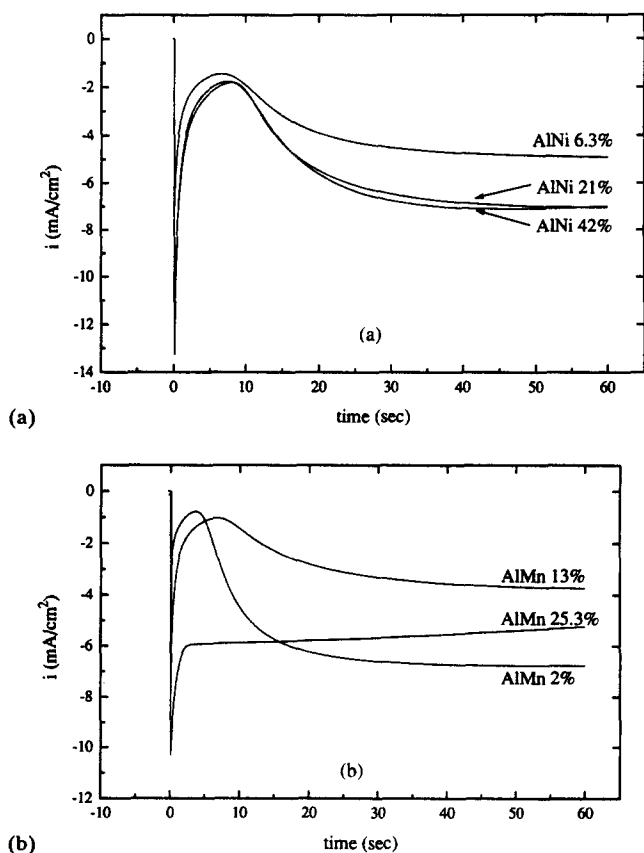

(a)

(b)

Fig. 2. (a) Potentiostatic transients for various AlNi substrates free of lithium (potential shift from rest potential to $E = 0$ mV vs. Li; 1 M LiClO₄/PC). (b) Potentiostatic transients for various AlMn substrates free of lithium (potential shift from rest potential to $E = 0$ mV vs. Li; 1 M LiClO₄/PC).

$$m = zF(c_{Li}^* - c_{Li}) \sqrt{\frac{D}{\pi}}$$ (2)

with,

$$(c_{Li}^* - c_{Li}) = c_0$$

where c_{Li}^* is the lithium concentration in the intermetallic compound, and c_{Li} the lithium concentration in the starting state.

The concentration gradient c_0 for the α-LiAl phase is given by:

$$c_0 = [c_{Li}(\alpha\text{-phase}) - c_{Li}(\text{pure-Al})]$$ (3)

$$c_0 = c_{Li}(\alpha\text{-phase}) = \frac{\rho_{\alpha-LiAl}}{M_{\alpha-LiAl}} x_{Li}$$ (4)

The concentration gradient for the β-LiAl phase is given by:

$$c_0 = [c_{Li}(\beta\text{-phase}) - c_{Li}(\alpha\text{-phase})]$$ (5)

Therefore, the diffusion coefficient is given by:

$$D = \left(\frac{m\sqrt{\pi}}{zFc_0}\right)^2$$ (6)

The concentration of lithium in the β-LiAl phase can also be estimated by X-ray measurements. For the intercalation of lithium into an aluminium foil (thickness 50 μm) at a constant current density ($i = 84$ μA/cm²) 65 h are necessary. During this time an amount of 2×10^{-4} mol lithium is deposited corresponding to a lithium concentration $c_0 = 4 \times 10^{-2}$ mol/cm³ [4].

Neglecting the charge of the double layer, Section I in Fig. 1(a) corresponds to the formation of nuclei of the α-LiAl phase. From the consumed charge during this period one can estimate the penetration depth of lithium towards the electrode surface assuming a homogeneous distribution of the lithium content. The consumed charge of 45 μC/cm² corresponds to 4.66×10^{-10} mol lithium dissolved in 1.75×10^{-8} mol aluminium in the α-LiAl stoichiometry. Pure aluminium crystallizes in a face centered cubic lattice with a lattice constant $a = 0.404$ nm [8]. Taking into account the surface of the electrode (0.2 cm²) lithium was penetrating 8.7 nm into the aluminium lattice (approximately 22 unit cells deep).

By means of this procedure we tried to estimate the diffusion behaviour of lithium for other binary aluminium alloys (Table 1). The estimated values for the product $c \sqrt{D}$ are shown in Table 2 for the pre-lithiated substrates investigated. It is obvious that a small addition of an inactive element increases the mobility of lithium especially at the grain boundaries. This effect can also be produced by the addition of grain finers such as strontium or boron [9].

Table 1

Summary of lithium diffusion data in various lithium inserting materials estimated by chronoamperometry. The substrates are free of lithium at the beginning of the measurement. Potential step from rest potential to $E=0$ mV vs. Li

Substrate	Intermetallic compound	Lithium contents (at.%)	Density (g/cm³)	$c_0\sqrt{D}\left(\dfrac{mol}{cm^2\sqrt{s}}\right)$	$D\left(\dfrac{cm^2}{s}\right)$
Bi	BiLi	48.6	7.39	9.3×10^{-8}	2.9×10^{-11}
Hg	Hg₃Li	21.4	12.3	4.9×10^{-7}	1.3×10^{-8}
Sn	Li₄Sn (Li₂₂Sn₅)	81.5	2.561	3.5×10^{-8}	1.5×10^{-8}
Pb	Li₃Pb	25.0	5.05	5.5×10^{-8}	9.8×10^{-11}
Al	α-AlLi	2.6	2.68	7.3×10^{-9}	7.9×10^{-12}
	β-AlLi	49.5	1.725	5.6×10^{-7}	6.0×10^{-10}
AlNi 6.3	α-AlLi	2.43		2.7×10^{-9}	1.2×10^{-12}
	β-AlLi	46.3		3.2×10^{-8}	2.3×10^{-12}
AlNi 21	α-AlLi	2.05		2.8×10^{-9}	1.8×10^{-12}
	β-AlLi	39.1		1.0×10^{-6}	3.3×10^{-9}
AlNi 42	α-AlLi	1.51		2.0×10^{-8}	1.8×10^{-10}
	β-AlLi	28.7		9.2×10^{-7}	4.9×10^{-9}
AlMn 2	α-AlLi	2.55		2.7×10^{-9}	1.1×10^{-12}
	β-AlLi	48.5		6.3×10^{-7}	7.8×10^{-10}
AlMn 13	α-AlLi	2.26		6.6×10^{-10}	8.6×10^{-14}
	β-AlLi	43.1		8.4×10^{-8}	1.8×10^{-11}
AlMn 25.3	α-AlLi	1.94		-6.5×10^{-9}	1.1×10^{-11}
	β-AlLi	36.9		1.7×10^{-7}	1.0×10^{-10}

Table 2

Summary of lithium diffusion data in various lithium inserting materials estimated by chronoamperometry: lithium has been plated before the measurement. (1 mAh/cm²; potential step from rest potential to $E=0$ mV vs. Li)

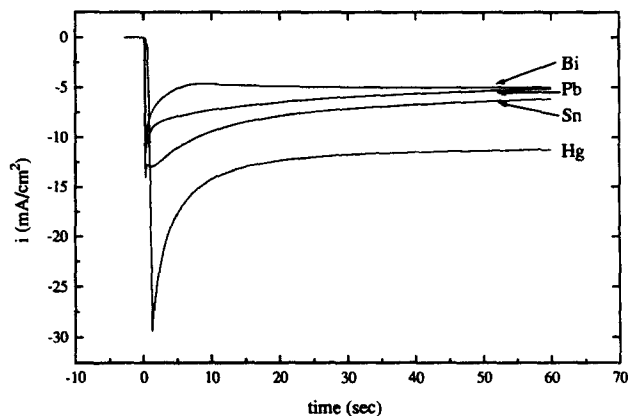| Substrate	$c_0\sqrt{D}\left(\dfrac{mol}{cm^2\sqrt{s}}\right)$	
	Volume diffusion	Grain-boundary diffusion
Al$_x$Li$_y$	1.7×10^{-8}	5.3×10^{-8}
(AlNi 6.3)$_x$Li$_y$	5.6×10^{-8}	2.4×10^{-7}
(AlNi 21)$_x$Li$_y$	1.1×10^{-7}	5.4×10^{-7}
(AlNi 42)$_x$Li$_y$	1.1×10^{-7}	6.7×10^{-7}
(AlMn 2)$_x$Li$_y$	2.1×10^{-8}	4.8×10^{-7}
(AlMn 13)$_x$Li$_y$	5.5×10^{-8}	2.6×10^{-7}
(AlMn 25.3)$_x$Li$_y$	5.3×10^{-8}	5.9×10^{-8}

Fig. 3. Potentiostatic transients for various lithium alloys substrates free of lithium (potential shift from rest potential to $E=0$ mV vs. Li; 1 M LiClO₄/PC).

3.2. Chronoamperometry on further lithium alloying substrates

In addition to the matrix alloys on basis of aluminium, a series of other elements forming lithium alloys have been investigated. Bismuth, mercury, tin and lead are well known to form easily lithium alloys. The potentiostatic current transients for these systems are shown in Fig. 3. The applied potential step was always chosen in a region where the lithium alloy could be formed.

All substrates show a 'normal' chronoamperometric behaviour. In these materials the lithium-containing phase is directly growing at the formed nuclei. No other slow process is occurring before. The capability of lithium incorporation is much more higher for these materials than it is in the case of the aluminium substrates, which can be conducted from cyclic voltammograms and the current–time transients. As expected, mercury shows the highest current densities during the insertion of lithium.

4. Conclusions

The mobility of lithium in an aluminium alloy depends on the grain-size distribution. Small additions of inactive (in response to lithium) elements increase the mobility of lithium especially at the grain boundaries.

References

[1] D. Billaud, E. MacRae and A. Herold, *Mater. Res. Bull.*, *14* (1979) 857.

[2] D. Fauteux and R. Koksbang, *J. Appl. Electrochem.*, *23* (1993) 1–10.

[3] D. Rahner, G. Ludwig, H. Bischoff, I. Hanke, S. Machill, K. Siury and K. Wiesener, *Wiss. Z. Technische Universität Dresden*, *41* (5) (1992) 52–60.

[4] I. Hanke, S. Machill, D. Rahner and K. Wiesener, *J. Power Sources*, *43/44* (1993) 421–427.

[5] B.N. Kabanov, I.I. Ashtakhov and I.G. Kiseleva, *Electrochim. Acta*, *24* (1979) 167.

[6] A.S. Baranski and W.R. Fawcett, *J. Electrochem. Soc.*, *129* (1982) 901–907.

[7] W. Schatt, *Einführung in die Werkstoffwissenschaft*, Deutscher Verlag für Grundstoffindustrie, Leipzig, 1974, pp. 193–195.

[8] P. Eckerlin and H. Kandler, *Landolt–Börnstein: Zahlenwerte und Funktionen aus Naturwissenschaft und Technik, Gruppe III: Kristall- und Festkörperphysik*, Band 6: *Strukturdaten der Elemente und intermetallischen Phasen*, Springer, Berlin, 1971.

[9] *Eur. Patent No. 0 574 555*.